

New Quality Assurance Algorithms for the DWD Polarimetric C-Band Weather Radar Network

Manuel Werner, Jörg Steinert

Deutscher Wetterdienst, Frankfurter Straße 135, 63067 Offenbach (Main), Germany,

manuel.werner@dwd.de, joerg.steinert@dwd.de

(Dated: May, 30th 2012)

1. Introduction

Nowadays, the assimilation and usage of weather radar data represents an important cornerstone in many meteorological applications like numerical weather prediction (NWP), quantitative precipitation estimation (QPE), and severe weather warning systems. Unfortunately, the benefit, especially in subsequent automated schemes, may be significantly spoiled by spurious radar echoes. Therefore, a real-time quality control of the radar data is mandatory.

In 2010 the Deutscher Wetterdienst (DWD) has started the exchange of its Doppler C-Band weather radar network with 17 dual-polarimetric EEC DWSR-5001C/SDP-CE radars. In association with this procedure, DWD has launched the internal project ‘Radarmaßnahmen’ with the aim to implement state-of-the-art dual-polarimetric algorithms and to redesign or improve existing methods for *weather radar monitoring, data quality control, hydrometeor classification, and quantitative precipitation estimation*. These new techniques are realized in a convenient software framework POLARA (Polarimetric Radar Algorithms), which is also newly developed and integrated into DWD’s operational radar data processing environment in the course of this project (Rathmann et al. (2012); this conference).

As an excerpt of this ongoing work, in this paper, recent developments of post-processing quality control algorithms for the new dual-polarimetric radars are presented. These advancements are consistent with the existing quality control strategy; cf. Hassler et al. (2006), Helmert et al. (2006, 2008, and 2012), and Hengstebeck et al. (2010). In particular, new methods for clutter and bright band detection, as well as propagation path attenuation correction are introduced.

The paper is organized as follows. In Chapter 2, the status quo of the operational radar data quality control scheme of the DWD is summarized. This represents the starting point for our work. The main Chapter 3 is then dedicated to the presentation of the new developments. For each algorithm, the principal functionality is briefly described, each followed by the results obtained for selected weather cases. The chapter finishes with a brief insight into the software technical realization of the new algorithms within the mentioned framework POLARA. The final Chapter 4 contains a conclusion and closes with a short outlook on future developments.

2. The radar data quality control concept of the DWD

This chapter provides a short outline of the present, operational radar data acquisition and quality assurance strategy applied in the German weather radar network.

2.1 Assembly of data in the radar network

DWD operates a network of 16 radar devices (17 after completion of network renewal) with a homogeneous scan strategy. Radar scans in five (‘precipitation scan’) and fifteen minute intervals (‘Doppler scan’ and ‘intensity scan’) are performed. The ‘precipitation scan’ (PRF 600 Hz, max. range 150 km) consists of the data recorded during a full revolution of the antenna with terrain-following low elevation angles. The ‘Doppler scan’ (dual PRF 800/1200 Hz, 124 km) consists of 18 *sweeps*, i.e., the respective data from a full antenna revolution, recorded with fixed elevation angles between 0.5° and 37°. The long-range ‘intensity scan’ (500 Hz, 256 km) collects five sweeps at different elevations between 0.5° and 4.5°.

An initial stage of quality control is performed at the radar itself in the signal processor. Here a set of filters and thresholds is applied. One building block in this filtering scheme is a *Doppler filter* for the removing of stationary clutter. For each sweep, the resulting pre-filtered moments, e.g., reflectivity and radial velocity, are coded in a separate file and transmitted in real-time to the central office in Offenbach via an automated file distribution service (AFD). Then, the gathered data sweeps undergo a second stage of post-processing quality control, on which this paper focuses.

2.2 The radar data quality control software RadarQS

The post-processing quality control to remove the spurious signals remaining after the filtering in the signal processor is currently performed using the DWD software package RadarQS, see Hengstebeck et al. (2010) for a detailed description. For each pre-filtered reflectivity and radial velocity sweep a corresponding separate quality product is generated. These products encode for each individual range bin a set of quality bits, where each bit refers to one quality relevant phenomenon. This includes *spoke and ring artifacts, clutter, second trip, and radial velocity aliasing*. Moreover, the software is designed to detect gross radar data errors affecting the whole sweep, e.g., corrupt datasets due to a possible temporary technical radar problem. To detect such errors, only the reflectivity and radial velocity data itself and no additional data are used.

Subsequent meteorological schemes are then equipped with the pre-filtered reflectivity and/or radial velocity data and the corresponding quality products. Each user may individually decide how to proceed in case a quality relevant event in a range bin or the whole sweep has occurred.

3. Development of new quality assurance algorithms for the dual-polarimetric radars

As mentioned in Chapter 1, the radar network exchange is accompanied by a supplementary project dealing with the development of new radar data processing algorithms tailored to the new dual-polarimetric devices. One principal working field herein is the further development and completion of the existing quality control algorithm chain realized in RadarQS (cf. Chap. 2.2), and the integration of all extended and newly developed methods into the new software framework POLARA (cf. Chap. 1).

In the sequel, three algorithms that have been recently developed in this context are presented. A brief glimpse at their realization in POLARA is given subsequent to that.

3.1 Clutter detection using dual-polarimetric data

Firstly, the important issue of clutter detection is addressed. Basically, one may distinguish between *stationary clutter*, which is defined to expose a radial velocity of approximately 0 m/s on the one hand, and between *variable clutter*, for which this assertion is not valid, on the other hand. The stationary clutter problem is initially treated by the Doppler filter in the signal processor. Such a filter has the ability to remove significant contributions of the Doppler spectrum close to 0 m/s. Weather signals, which are assumed to propagate with a radial velocity different from zero, are preserved. Hence, the advantage is that, in principle, clutter echoes superimposed on weather echoes can be separated within a range gate, preserving only the desired meteorological part. However, it is known that this methodology has its weaknesses (Seltmann (2000)). For instance, precipitation echoes along the line perpendicular to the dominating wind direction may expose a radial velocity close to 0 m/s, and thus are often erroneously biased. From these preliminary remarks, the following requirements for our post-processing scheme can be deduced.

a) Requirements for the algorithm

The post-processing clutter algorithm is intended to

- detect stationary clutter (0 m/s radial velocity, e.g., buildings, mountains, etc.),
- detect variable clutter (birds, insects, chaff, etc.),
- check the performance of the Doppler filter previously applied in the signal processor,

and encode for each range gate the result in the corresponding quality product by activating a respective quality bit. The Doppler filter check supplies the information whether the Doppler filter has rightly worked or if it has falsely biased a meteorological signal.

b) Structure of the algorithm

The method is designed as a three-step procedure and essentially relies on *horizontal reflectivity*, *differential reflectivity*, *horizontal radial velocity*, *differential phase*, *co-polar correlation coefficient* measurements, and the *Doppler filter correction of the horizontal reflectivity*.

The **first main step** consists in a fuzzy logic classification as described in Schuur et al. (2003) to initially map each range gate to one of the classes *meteorological*, *ground clutter/anomalous propagation*, or *biological*. The approach is based on a subset of the mentioned parameters, namely the horizontal reflectivity (including a derived texture parameter), the differential reflectivity, and the co-polar correlation coefficient. The utilization of the differential phase as suggested in Schuur et al. (2003) is decoupled from this classification procedure and comes into play in the second main step.

In the **second main step**, the result of the performed classification is confronted with the information extracted from a ray-wise calculated texture parameter derived from the differential phase. In fact, the differential phase data of meteorological echoes along one ray exposes a rather smooth structure, whereas for underlying significant clutter echoes, or clear air, one usually observes an irregular, noisy pattern. The ray-wise texture parameter is computed as follows. We take a local boxcar standard deviation of the samples of the second derivative of an approximating spline (de Boor (2001)) fitted to the differential phase data. At range gates where the original differential phase data is irregular, the standard deviation should be large, i.e., it should exceed a certain threshold. The smooth meteorological regions induce a small standard deviation, less than the threshold. Note that we use the second derivative of the spline, because the irregular, noisy parts are even more enhanced, so that the separation from the smooth areas becomes easier. For each range bin, the decision, i.e., meteorological (small standard deviation) or non-meteorological (large standard deviation), is then confronted with the classification from the previous main step. In case of a contradicting result, the outcome of the classification wins, only if the probability of the respective class is sufficiently high. If, after all, the final decision results in clutter, the unfiltered radial velocity (prior to Doppler filtering in signal processor) is used to conclude whether the clutter is stationary or variable. At the end of main step two, one of the quality bits `bit_meteorological`, `bit_stationary_clutter`, `bit_variable_clutter`, or as a subclass of the latter, `bit_biological` is activated in the quality products for the reflectivity and the radial velocity.

The **third and final main step** contains the inspection of the Doppler filter performance. In case the result after main step two for a range bin is meteorological (`bit_meteorological` active), the Doppler filter corrected radial velocity is close to zero, but the Doppler filter correction in dB exceeds a certain bound, it is assumed that the Doppler filter has struck inadmissibly. Otherwise, if the result after step two is stationary clutter (`bit_stationary_clutter` active), and the Doppler filter correction in dB has been significant, the Doppler filter has validly worked. These information are also encoded in the corresponding quality product by activating a respective separate quality bit.

c) Results for an example weather case

An example weather case from the dual-polarimetric DWD radar Offenthal near Frankfurt (Main) on September, 4th 2011, 01:20 UTC, ‘precipitation scan’ mode, is shown in Fig. 1. It visualizes the reflectivity and radial velocity data and the differential phase. Moreover, the thresholded texture parameter derived from the differential phase introduced in *b)* is depicted. Figure 2 contains the azimuth-range plot of the quality product contents corresponding to the horizontal reflectivity (with signal processor filters applied) after main step two, prior to the Doppler filter check. Moreover, the Doppler filter control bits, set by step three, are shown (Fig. 2, middle and right picture).

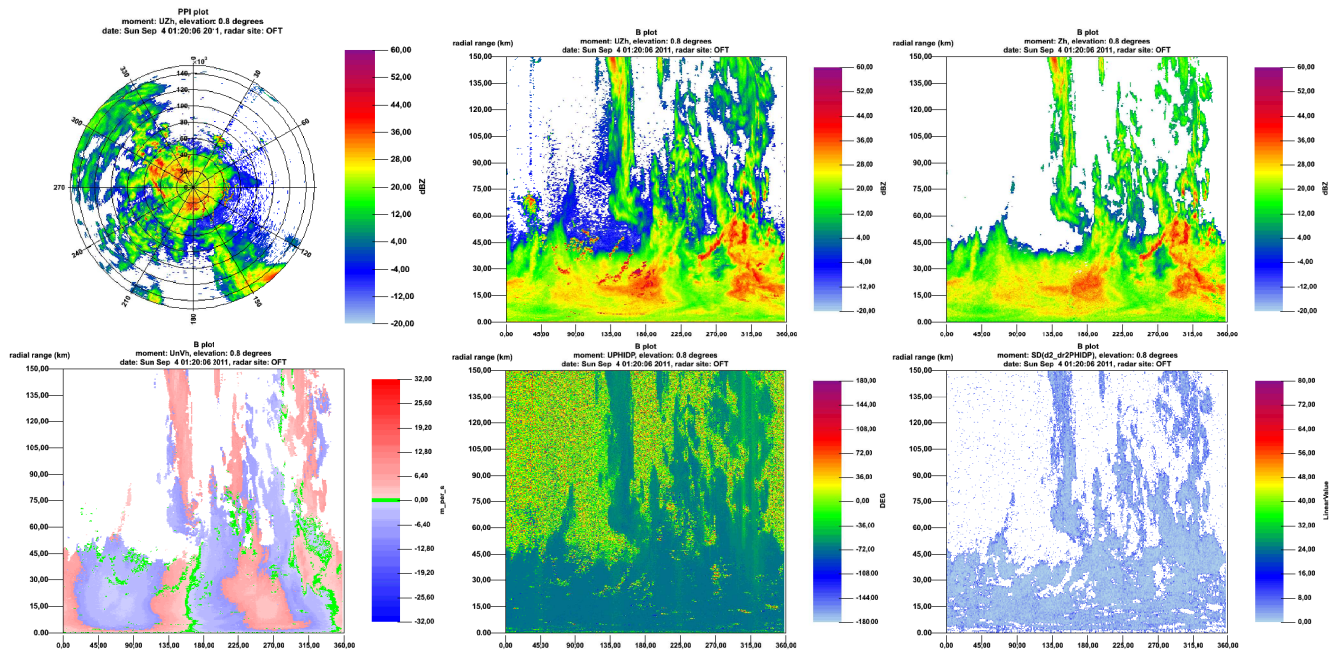


*Fig. 1 Example from DWD radar Offenthal, September, 4th 2011, 01:20 UTC, ‘precipitation scan’. **First Row:** PPI and azimuth-range plots of unfiltered reflectivity (no signal processor filters applied), azimuth-range plot of reflectivity after application of signal processor filters. **Second Row:** Azimuth-range plots of unfiltered radial velocity (Nyquist velocity 7,95 m/s), differential phase, and texture parameter derived from differential phase as described in *b)*.*

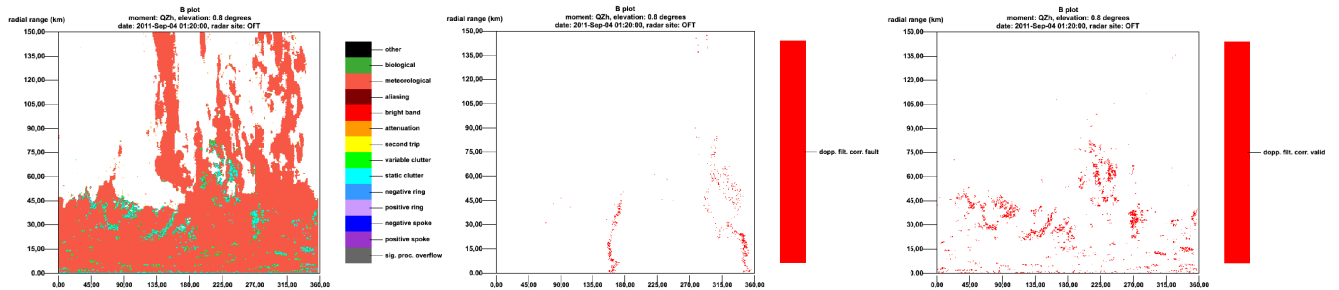


*Fig. 2 **Left:** Azimuth-range plot of quality product after main step two corresponding to the pre-filtered reflectivity from Fig. 1, upper right. **Middle:** Range gates inadmissibly filtered by Doppler filter. **Right:** Admissibly Doppler filtered pixels.*

3.2 Detection of the bright band

A main subject of radar meteorology is the quantitative precipitation estimation. Straight forward procedures to get the correct amount of precipitation are interfered, among other quality issues, like the aforementioned clutter detection, by the so-called bright band. Apart from the improvement of the QPE, the bright band detection also enhances a subsequent hydrometeor classification. This double-sided character is due to the fact that especially in the bright band melting particles are present that are forming a separate hydrometeor class. These melting particles lead to an increase of the radar reflectivity during the melting process (e.g., Steinert et al. (2010)). The consequence is overestimation in the QPE. The bright band detection introduced in the following is individually applied to the PPI scans from the different DWD radar sites.

a) Prerequisites for the algorithm

Because of the melting behavior, a relation of the bright band to the air temperature is obvious, leading to the temperature as input parameter. In particular, at this stage of the development, the height of the 0°C isotherm and the height of the snow limit are used. Both are computed within the COSMO-DE NWP model.

Usually, the bright band detection is not done for near-ground elevations (e.g., Giangrande et al. (2008)). Reasons are the reducing of misinterpretations from clutter or other quality phenomena and the ‘sharper’ designation of the bright band at higher elevations. To enhance the estimation of the bright band for the low elevation angles of the ‘precipitation scan’ (see

Chap. 2.1) a bright band history was introduced. This history includes the detection results of the preceding ‘Doppler scans’ and ‘intensity scans’ and are therefore predominantly created from measurements with higher elevations.

Furthermore, the results of previously processed quality assurance algorithms, namely the spoke detection and the aforementioned clutter detection, are taken into account for the estimation of the bright band. At this stage, the data of range bins affected with poor quality were filtered and therewith dropped out for later analysis.

To summarize, the input for the bright band detection is formed by the above mentioned parameters together with the available radar measurements of the reflectivity (Z_h), differential reflectivity (Z_{dr}) and co-polar correlation coefficient (ρ_{hv}). The algorithm is realized in such a way that just Z_h is mandatory. This means, the algorithm also works with single-polarimetric radar data. However, the best performance is attained with a complete set of input parameters.

b) Building blocks of the detection algorithm

The estimation of the bright band is separated in three main parts.

Firstly, in the **pre-processing** stage, the input parameters are tested for validity and prepared for further processing. Here, one step is the transformation of the data containing absolute height information above mean sea level (like the bright band history and the height of the 0°C isotherm) to relative heights related to the radar measurements.

The **processing** part consists of a standard fuzzy classifier handling every single input parameter with associated membership functions. The membership functions for the radar measurements are adapted versions of the trapezoidal functions of Boodoo et al. (2010). If a parameter, except for Z_h , is missing, the weighting factor for the membership function is set to 0. The estimation of the correct values for the adjusting screws of the fuzzy classifier is still in progress.

After that, a **post-processing** part is added. Here, the detection along one ray and between neighboring rays is connected to improve the result. This proceeding is based on the idea of a smooth bright band with slightly areal variations within the coverage of one weather radar. As one step, the averaging of a 21° azimuth sector, as in Giangrande et al. (2008), is implemented. In addition, the detection result is encoded in the quality products by activating the appropriate quality bit.

c) Example dataset

To give an impression of the bright band detection, one example with data recorded on March, 7th 2012, 22:45 UTC, is shown in Fig. 4. In addition, Fig. 3 gives the contributing radar measurements, namely Z_h , Z_{dr} and ρ_{hv} . The chosen dataset is a near-ground ‘precipitation scan’ from the radar site Offenthal, near Frankfurt (Main).

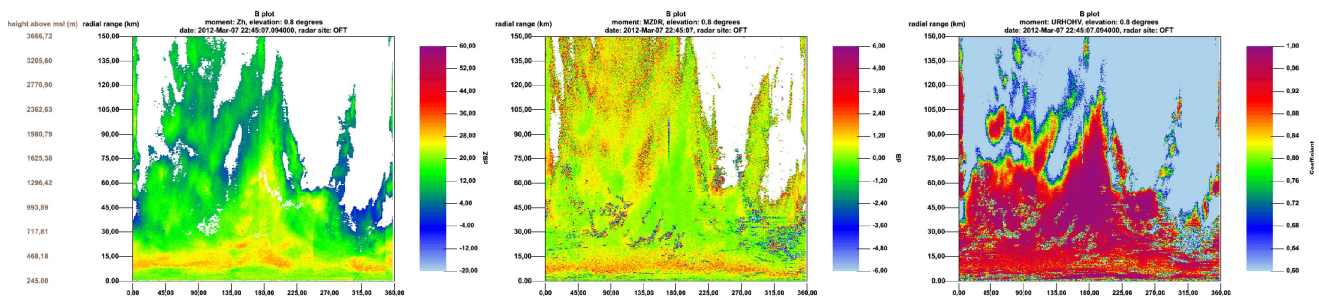


Fig. 3 Example dataset from radar Offenthal, March, 7th 2012, 22:45 UTC. Azimuth-range plot of **left**: signal processor filtered reflectivity, **middle**: uncorrected differential reflectivity, **right**: uncorrected co-polar correlation.

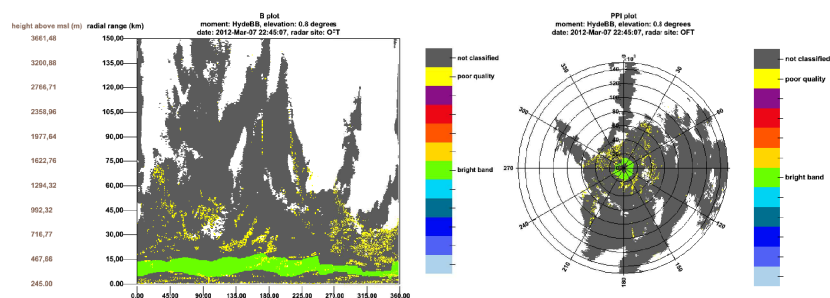


Fig. 4 Bright band detection of the dataset introduced in Fig. 3. On the **left** hand side the azimuth-range plot and on the **right** hand side the same data as PPI is displayed. The bright band class is plotted in green color and the poor quality marked ranged bins, that are related to the clutter detection (Chap. 3.1), are presented in yellow color.

3.3 Attenuation correction

The detection and correction of propagation path attenuation represents another important component in weather radar quality control systems. The accuracy of hydrometeor classification and quantitative precipitation estimation schemes hinges on the availability of attenuation corrected reflectivity and differential reflectivity data. However, the quality control software RadarQS used up to now does not contain a scheme for this purpose. This gap is filled by the new polarimetric algorithm described below.

a) Design of the algorithm

The algorithm realized in the new DWD software package POLARA relies on the self-consistent Φ_{dp} constraint method described in Bringi et al. (2001), which is based on a rain profiling scheme proposed by Testud et al. (2000). The starting point is the model power law relation $A_h(r) = a[\zeta_h(r)]^b$, and the linear model equation $A_h(r) = \alpha K_{dp}(r)$, in which the specific attenuation $A_h(r)$ at range r is in dB/km, $\zeta_h(r)$ is the intrinsic horizontal reflectivity in mm^6/m^3 , and $K_{dp}(r)$ represents the specific differential phase. Using this model, for a given α , the specific attenuation $A_h(r; \alpha)$ may be expressed in terms of the measured reflectivity value $z_h(r)$ (in linear scale) and $\Delta\Phi_{dp} = \Phi_{dp}(r_m) - \Phi_{dp}(r_0)$, i.e., the variation of the differential phase from a range location r_0 in front of a rain cell to a location r_m beyond, see Bringi et al. (2001) for details. To take account of the sensitivity of the proportionality parameter α to temperature and drop size distribution, Bringi et al. (2001) suggest calculating a reconstructed Φ_{dp} profile $\Phi_{dp}^{rec}(r) := 2 \int_{r_0}^r \frac{A_h(s; \alpha)}{\alpha} ds$ for different choices of α . The idea is then to compare $\Phi_{dp}^{rec}(r)$ with a filtered version of the measured profile. The final result for the specific attenuation is set to $A_h(r; \alpha_{opt})$, where α_{opt} is the factor for which the distance between the reconstructed and the filtered original Φ_{dp} profile is minimal. Finally, the corrected horizontal reflectivity in dBZ is obtained by $10 \log_{10}(\zeta_h(r)) = 10 \log_{10}(z_h(r)) + 2 \int_{r_0}^r A_h(s; \alpha_{opt}) ds$. The pre-smoothing of the differential phase profile is performed using the iterative filtering scheme proposed in Hubbert et al. (1995). Instead of a FIR filter as in Hubbert et al. (1995), a smoothing spline (de Boor (2001)) is applied. The correction of the differential reflectivity Z_{dr} for differential attenuation is performed using the Z_{dr} constraint approach described in Bringi et al. (2001), §7.4.2 (iii). Moreover, the algorithm is performed for connected ray segments of common hydrometeor type, provided by a hydrometeor pre-classification scheme, which has also been realized in POLARA.

The calculated local and accumulated specific and differential attenuation, and the respective corrected moments are passed to subsequent algorithms by writing these data to file or via an internal data structure. In addition, the range gates, for which the specific attenuation is significant, are marked in the quality products for reflectivity and radial velocity.

b) An example weather case

A model weather situation at the polarimetric radar site Offenthal on June, 22nd 2011, 12:30 UTC, ‘intensity scan’ mode, is considered in Fig. 5. During this convective event, considerable attenuation effects have occurred.

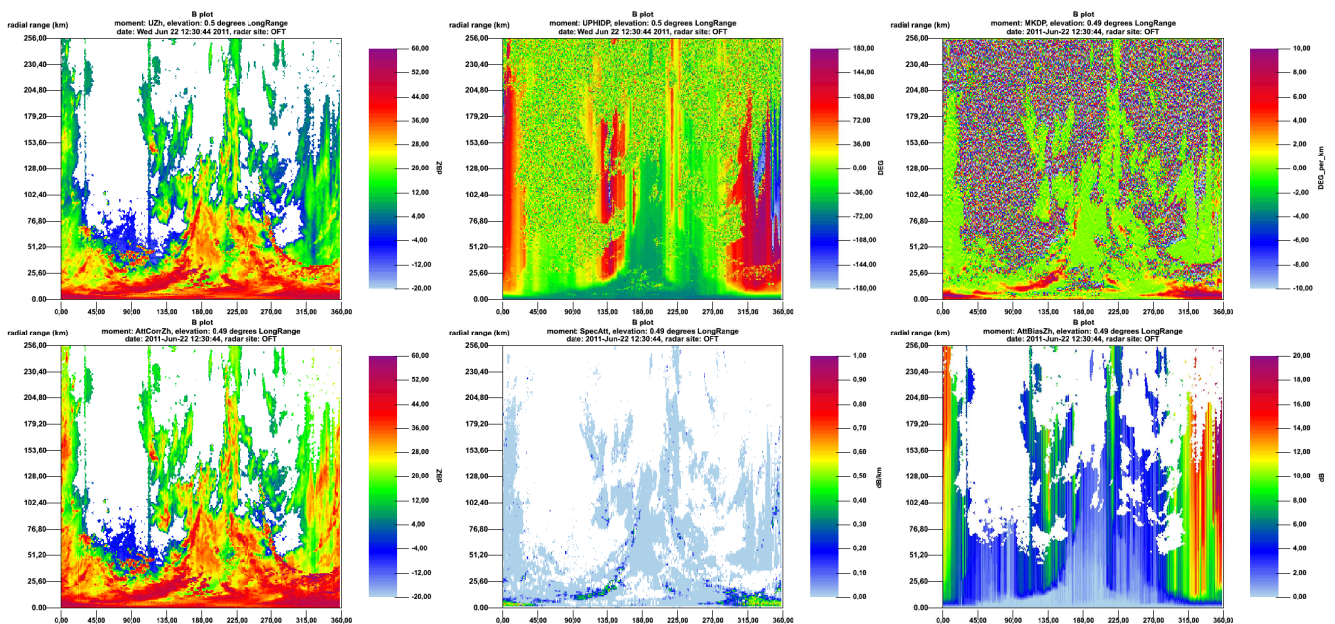


Fig. 5 Example from DWD radar Offenthal, June, 22nd 2011, 12:30 UTC, ‘intensity scan’. **First Row:** Azimuth-range plots of unfiltered reflectivity (no signal processor filters applied), differential phase, and specific differential phase.

Second Row: Azimuth-range plots of unfiltered (no signal processor filters applied) reflectivity corrected for attenuation, the calculated specific attenuation, and the resulting cumulative attenuation.

3.4 Realization of the methods in the new software POLARA (Polarimetric Radar Algorithms)

The algorithms described in the Chapters 3.1-3.3 have been realized in the software framework POLARA (cf. Rathmann et al. (2012); this conference). The virtue of POLARA is twofold. On the one hand, it provides a convenient environment for the development of post-processing algorithms, providing a generic algorithm interface, radar data file I/O components, an internal radar data model, and configuration and logging interfaces. On the other hand, a runtime environment for the permanent 24/7 processing of radar data is available, including an easy mechanism to integrate a new method into the chain of permanently running schemes.

The sequence of post-processing quality control algorithms for each station in the new radar network, i.e., after the renewal, will be subsequently performed in a separate 'job' (executable) within the mentioned runtime environment. These jobs (17 in number) are started and monitored by a special scheduler program. Moreover, they are supplied with the relevant radar data by an automated radar data file managing process. The scheduler and radar data file manager processes represent the core parts of the POLARA runtime environment (Rathmann et al. (2012); this conference).

4. Conclusion and outlook

Post-processing quality control algorithms for the new dual-polarimetric radars in the DWD network have been introduced, including clutter and bright band detection, as well as propagation path attenuation correction. These methods are implemented within the new software package POLARA currently being developed at the DWD. The existing radar data quality assurance strategy is maintained. The development of POLARA and the algorithms therein is still in progress. When this stage is completed, POLARA is intended to become operational and so to take on the job currently done by RadarQS.

Until then, the mentioned algorithms are going to be extensively tested, tuned, and further developed. Moreover, a systematic verification of their accuracy as far as possible is an open working task.

References

- Boodoo S., Hudak D., Donaldson N., Leduc M., 2010: Application of dual-polarization radar melting-layer detection algorithm. *J. Appl. Meteor. Climatol.*, **49**, 1779–1793.
- Bringi V.N., Chandrasekar V., 2001: Polarimetric Doppler Weather Radar. *Cambridge University Press*.
- de Boor C., 2001: A Practical Guide to Splines. *Springer, New York*.
- Giangrande S.E., Krause J.M., Ryzhkov A.V., 2008: Automatic designation of the melting layer with a polarimetric prototype of the WSR-88D radar. *J. Appl. Meteor. Climatol.*, **47**, 1354–1364.
- Hassler B., Helmert K., Seltmann J., 2006: Identification of spurious precipitation signals in radar data. *Proc. 4th Europ. Conf. On Radar in Meteor. and Hydrol.*, 18–22 September 2006, Barcelona, Spain (Göttingen: Copernicus GmbH), ERAD Publication Series 3, 590–592.
- Helmert K., Hassler B., 2006: Development and application of a quality-index composit. *Proc. 4th Europ. Conf. On Radar in Meteor. and Hydrol.* 18–22 September 2006, Barcelona, Spain (Göttingen: Copernicus GmbH), ERAD Publication Series 3, 587–589.
- Helmert K., Hengstebeck T., Seltmann J., 2008: DWD's operational tool to enhance radar data quality. *Proc. 5th Europ. Conf. On Radar in Meteor. and Hydrol.*, Helsinki, Finland.
- Helmert K., Hassler B., Seltmann J., 2012: An operational tool to quality control 2D radar reflectivity data for assimilation in COSMO-DE. *International Journal of Remote Sensing*, **33**, 3456–3471.
- Hengstebeck T., Helmert K., Seltmann J., 2010: RadarQS - a standard quality control software for radar data at DWD. *Proc. 6th Europ. Conf. On Radar in Meteor. and Hydrol.*, Sibiu, Romania.
- Hubbert J., Bringi V.N., 1995: An iterative filtering technique for the analysis of copolar differential phase and dual-frequency radar measurements. *J. Atmos. Oceanic Technol.*, **12**, 643–648.
- Rathmann N., Mott M., 2012: Effective radar algorithm software development at the DWD. *Proc. 7th Europ. Conf. On Radar in Meteor. and Hydrol.*, ext. abs. no. **316**, Toulouse, France.
- Schuur T., Ryzhkov A.V., Heinselman P., 2003: Observations and classification of echoes with the polarimetric WSR-88D radar. *NOAA/NSSL Report*, 45 pp.
- Seltmann J., 2000: Clutter versus radar winds. *Phys. Chem. Earth*, **B25**, 1173–1178.
- Steinert J., Chandra M., 2010: Melting-layer modeling at C-band. *Adv. Radio Sci.*, **8**, 285–288.
- Testud J., Bouar E. L., Obligis E., Ali-Mehenni M., 2000: The rain profiling algorithm applied to polarimetric weather radar. *J. Atmos. Oceanic Technol.*, **17**, 332–356.